

Anionic Polymerization of (Meth)acrylates in the Presence of Tetraalkylammonium Halide–Trialkyl Aluminum Complexes in Toluene, 1. Kinetic Investigations with Methyl Methacrylate

Helmut Schlaad and Axel H. E. Müller*

Institut für Physikalische Chemie, Universität Mainz, Welterweg 15, D-55099 Mainz, Germany

Received December 23, 1997; Revised Manuscript Received July 27, 1998

ABSTRACT: The anionic polymerization of methyl methacrylate in toluene in the presence of tetraalkylammonium–trialkylaluminum 1:2-complexes, $\text{NR}_4^+[\text{Al}_2\text{R}'_3\text{X}]^-$, has living and controlled character up to -20°C . Quantitative monomer conversions are usually reached within a few minutes. The resulting polymers have narrow molecular weight distributions ($1.05 < \bar{M}_w/\bar{M}_n < 1.20$) and are highly syndiotactic ($rr \approx 0.75$). Kinetic studies show that the mechanism of the polymerization is rather complex, implying an equilibrium between three active species of different reactivities.

Introduction

Recently, we elucidated the anionic polymerization of methyl methacrylate (MMA) with lithiated initiators in the presence of aluminum alkyls in toluene. The polymerization was shown to have living character, but it deviates from conventional first-order kinetics, and the polymers have fairly broad molecular weight distributions ($\bar{M}_w/\bar{M}_n > 1.5$).¹ On the basis of ^{13}C NMR measurements² and ab initio (density functional theory) quantum-chemical calculations,^{3,4} the structure of the active species is considered to be an ester enol aluminate, **1a**, which is in equilibrium with a less reactive dimeric associate, **1b** (Scheme 1).

The poor control of the polymerization was found to result from the formation and precipitation of a coordinative polymer network, in which in-chain ester carbonyl groups are coordinated to the lithium gegenion of the living chain end.⁵ The network formation could be suppressed by adding Lewis bases, e.g., esters or crown ethers, and then we obtained linear first-order time–conversion plots and PMMAs with narrow molecular weight distributions ($\bar{M}_w/\bar{M}_n < 1.3$) up to 0°C .³

In a different approach to prevent the network formation, we aimed at the exchange of the lithium ion by a less electropositive cation, e.g., a tetraalkylammonium ion. Usually, tetraalkylammonium halides (NR_4X) hardly dissolve in toluene, but according to Ziegler et al.,⁶ they give hydrocarbon-soluble complexes with aluminum alkyls (AlR'_3), $\text{NR}_4^+[\text{Al}_n\text{R}'_{3n}\text{X}]^-$ ($n = 1, 2$). In the complex with $n = 2$ the halogen forms a bridge between the two Al atoms.⁷ When we used ethyl α -lithioisobutyrate (EiBLi) in the presence of these complexes as initiator for the polymerization of MMA in toluene at 0°C , we quickly reached quantitative monomer conversions and polymers with unimodal and narrow molecular weight distributions ($\bar{M}_w/\bar{M}_n = 1.1$).^{8,9} In the absence of the aluminum alkyl, however, the polymerization has no controlled character at all.¹⁰ These results suggest that tetraalkylammonium halide–aluminum alkyl complexes support a living and controlled polymerization of MMA in toluene.

At this point, we describe the effect of tetraalkylammonium halide–aluminum alkyl complexes, especially that of the 1:2-complex $\text{NBu}_4^+[\text{Al}_2\text{Et}_6\text{Br}]^-$, on the po-

lymerization kinetics of MMA and on the molecular weight distributions and tacticities of the resulting polymers.

Experimental Section

Reagents. Ethyl α -lithioisobutyrate (EiBLi) was prepared according to the method of Lochmann and Lím.¹¹ Triethylaluminum (AlEt_3) was purchased from Aldrich as a 25 wt % solution in toluene and used as received. Tetraalkylammonium halides (NMe_4Cl , NEt_4Cl , NBu_4Cl , NBu_4Br , and NBu_4I) were purchased from Aldrich and freeze-dried from benzene. Methyl methacrylate (MMA, BASF AG) was fractionated from CaH_2 over a 1 m column filled with Sulzer packing at 45 mbar, stirred over CaH_2 , degassed, and distilled in a high vacuum. Toluene (BASF AG) was fractionated over a 1.5 m column, stirred twice over Na/K alloy, degassed, and distilled in a high vacuum. Octane (Aldrich) as internal standard for GC was stirred over Na/K alloy, degassed, and distilled in a high vacuum.

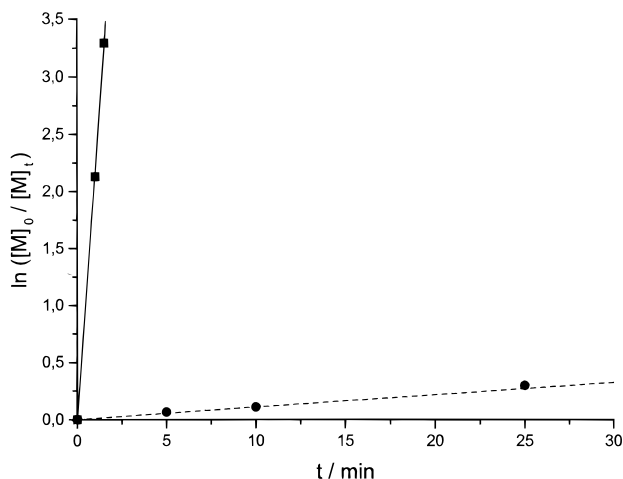
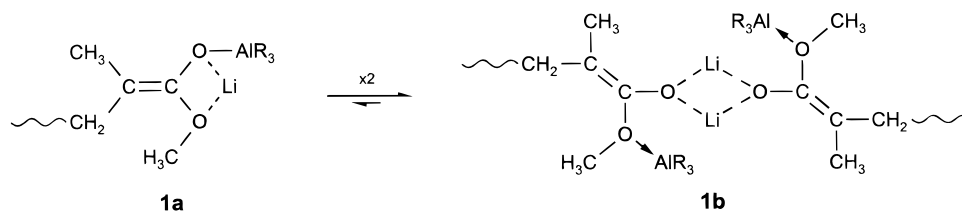
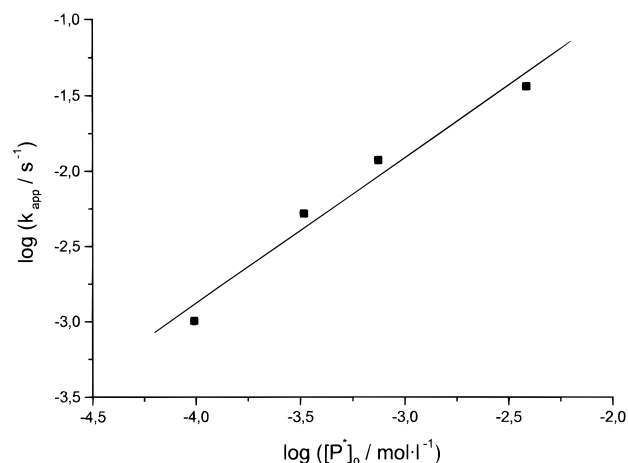
Kinetics. All experiments were carried out in a stirred tank reactor under nitrogen atmosphere. The initiator was prepared by adding ethyl α -lithioisobutyrate to a solution of the tetraalkylammonium halide–aluminum alkyl complex in toluene at the later polymerization temperature. The solution was stirred for 5 min, and then the monomer was added. The polymerization was quenched with methanol, and monomer conversion was determined with GC using octane as internal standard. After evaporation of the solvent, the polymer was dissolved in benzene, filtered, and freeze-dried.

GPC. GPC was performed using THF as the eluent at a flow rate of 1 mL/min. Detectors: 2 x JASCO–UVIDEC 100 III with variable wavelength and Bischoff RI detector 8110, column set: 2×60 cm, 5μ PSS SDV gel, 100 Å and linear, 10^2 – 10^5 Å. PMMA standards were used for calibration.

NMR. ^1H NMR spectra of the polymers were recorded with a Bruker AM-400 spectrometer at room temperature in CDCl_3 . The α -CH₃ signals were used for the determination of triad tacticities.

Results and Discussion

Compared to the anionic polymerization of MMA with EiBLi/ AlEt_3 in a 3:1 toluene/methyl pivalate v/v mixed solvent,³ the rate of propagation is about 2 orders of magnitude higher when we use EiBLi in the presence of $\text{NBu}_4^+[\text{Al}_2\text{Et}_6\text{Br}]^-$ in toluene (cf. Figure 1), and a polymer gel does not precipitate either. Both observations seem to indicate that the active species carries a tetrabutylammonium rather than a lithium gegenion (cf.

Scheme 1. Equilibrium between Unimeric and Dimeric Chain Ends in the Presence of AlR_3 **Figure 1.** First-order time-conversion plots for the anionic polymerization of MMA at $-20\text{ }^{\circ}\text{C}$ with $\text{EtBLi}/\text{AlEt}_3$ in 3:1 toluene/methyl pivalate v/v (●) and $\text{EtBLi}/\text{NBu}_4^+[\text{Al}_2\text{Et}_6\text{Br}]^-$ in toluene (■). $[\text{EtBLi}]_0 = 4.5 \times 10^{-3}\text{ mol/L}$, $[\text{NBu}_4\text{Br}] = 6.9 \times 10^{-3}\text{ mol/L}$, $[\text{AlEt}_3] = 15.0 \times 10^{-3}\text{ mol/L}$, and $[\text{MMA}]_0 = 0.233\text{ mol/L}$.**Figure 2.** Determination of the reaction order with respect to the concentration of active centers, $[\text{P}^*]_0$, for the anionic polymerization of MMA at $-20\text{ }^{\circ}\text{C}$ with $\text{EtBLi}/\text{NBu}_4^+[\text{Al}_2\text{Et}_6\text{Br}]^-$ in toluene. $[\text{EtBLi}]_0 = (0.16\text{--}4.04) \times 10^{-3}\text{ mol/L}$, $[\text{NBu}_4\text{Br}] = 6.9 \times 10^{-3}\text{ mol/L}$, $[\text{AlEt}_3] = 15.0 \times 10^{-3}\text{ mol/L}$, and $[\text{MMA}]_0 = 0.233\text{ mol/L}$. Slope: 1.0 ± 0.1 .

Introduction). However, the rate of propagation is considerably lower than one would expect for an active species with a large tetrabutylammonium gegenion.¹²

Ab initio (DFT) quantum-chemical calculations⁴ on the model compound $\text{EtBLi-NMe}_4^+[\text{AlMe}_3\text{Br}]^-$ provide **2a** and its dimeric associate **2b** as possible structures of the active species (Chart 1). Either species carries a tetraalkylammonium gegenion, but the lithium ion is still coordinated to the enolate oxygen and, in addition, to a trialkylaluminum halide anion. It appears that the gegenion of the active species might not be simply exchanged as expected at first.

Anyway, the polymerization usually follows first-order kinetics at $-20\text{ }^{\circ}\text{C}$, and the number-average degree of polymerization, P_n , increases linearly with monomer

conversion, x_p (see below). The resulting PMMAs have narrow molecular weight distributions ($1.05 < \bar{M}_w/\bar{M}_n < 1.20$) and, relying on GPC analysis with UV detection at $\lambda = 300\text{ nm}$, they are free of cyclic β -ketoester units. All these findings suggest that neither termination via back-biting nor transfer reactions occur; i.e., the polymerization has both living and controlled character. The initiator efficiency, f , is in the range 60–80% (cf. Table 1).

Further kinetic studies show that the reaction is first order with respect to the concentration of active centers, $[\text{P}^*]_0 = f[\text{EtBLi}]_0$ (Figure 2), and the initial concentration of the monomer, $[\text{MMA}]_0$.⁸ Assuming that the curvature in Figure 2 is not accidental would imply a change in reaction order for $[\text{P}^*]_0$ from 1.4 to 0.7, which is difficult to explain.

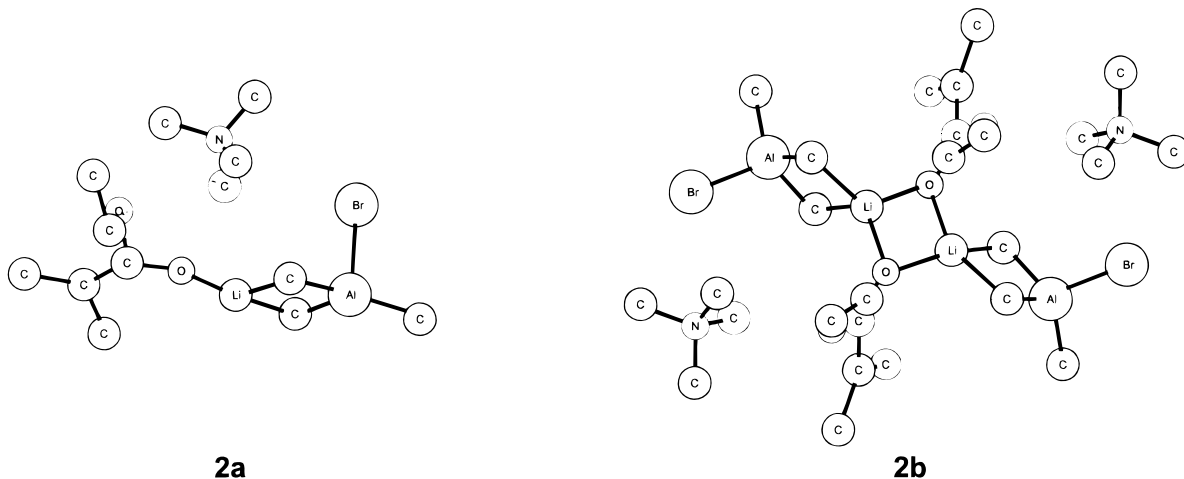
Chart 1. Calculated Structures of the $\text{EtBLi-NMe}_4^+[\text{AlMe}_3\text{Br}]^-$ Adduct (Unimer and Dimer)

Table 1. Molecular Weight Distributions and Tacticities of the Polymers Obtained from the Anionic Polymerization of MMA with $\text{EiBLi}/\text{NR}_4^+[\text{Al}_2\text{Et}_6\text{X}]^-$ in Toluene^c

NR ₄ X	T/°C	<i>t</i> _{max} /min	<i>x</i> _p at <i>t</i> _{max}	\bar{P}_n	\bar{P}_w/\bar{P}_n	<i>f</i>	tacticity			
							<i>mm</i>	<i>rr</i>	<i>r</i>	ρ
NMe ₄ Cl	-20	40	0.95	760	1.17	0.64	0.01	0.74	0.865	0.93
NEt ₄ Cl	-20	18	1	660	1.12	0.82	0.02	0.72	0.850	0.98
NBu ₄ Cl	-20	15	1	890	1.08	0.59	0.01	0.76	0.875	0.95
NBu ₄ Br	-20	13	1	690	1.06	0.74	0.01	0.73	0.860	0.93
NBu ₄ I	-20	25	0.81	1000	1.12	0.42	0.01	0.72	0.855	0.93
NBu ₄ Br	-78 ^a	390	0.31	220	1.09	0.72	0.02	0.72	0.850	0.98
NBu ₄ Br	-58	180	0.89	560	1.10	0.77	0.01	0.77	0.880	0.96
NBu ₄ Br	-38	70	1	645	1.07	0.74	0.01	0.75	0.870	0.94
NBu ₄ Br	-20	13	1	690	1.06	0.74	0.01	0.73	0.860	0.93
NBu ₄ Br	0 ^b	5	0.89	620	1.26	0.67	0.03	0.66	0.815	0.97
NBu ₄ Br	+20 ^b	4	0.20	275	1.39	0.37	0.04	0.61	0.785	0.96

^a Precipitation of a polymer gel; $\bar{M}_n = 12\,400$, and $\bar{M}_w/\bar{M}_n = 1.77$. ^b Downward curvature of first-order time-conversion plot indicates termination reactions. ^c $[\text{EiBLi}]_0 \approx 0.44 \times 10^{-3}$ mol/L, $[\text{NR}_4\text{X}] = 6.9 \times 10^{-3}$ mol/L, $[\text{AlEt}_3] = 15.0 \times 10^{-3}$ mol/L, $[\text{MMA}]_0 = 0.233$ mol/L. *x*_p: monomer conversion. \bar{P}_n : number-average degree of polymerization. \bar{P}_w/\bar{P}_n : polydispersity index. *f*: initiator efficiency. ρ : persistence ratio, $2\langle m \rangle \langle r \rangle / \langle mr \rangle$.

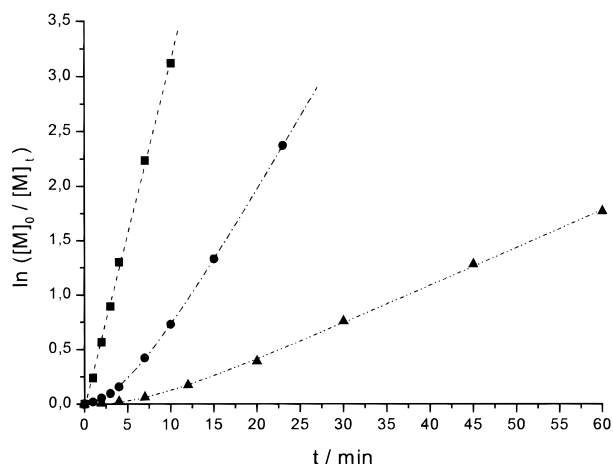


Figure 3. First-order time-conversion plots for the anionic polymerization of MMA at -20 °C with $\text{EiBLi}/\text{NBu}_4^+[\text{Al}_2\text{Et}_6\text{Br}]^-$ in toluene for different concentrations of $\text{NBu}_4^+[\text{Al}_2\text{Et}_6\text{Br}]^-$. $[\text{EiBLi}]_0 = 0.44 \times 10^{-3}$ mol/L; $[\text{NBu}_4\text{Br}]/[\text{AlEt}_3] = (0.5/1.1)$ (---▲---), $(1.2/2.5)$ (---●---), and $(6.9/15.0) \times 10^{-3}$ mol/L (---■---); and $[\text{MMA}]_0 = 0.233$ mol/L.

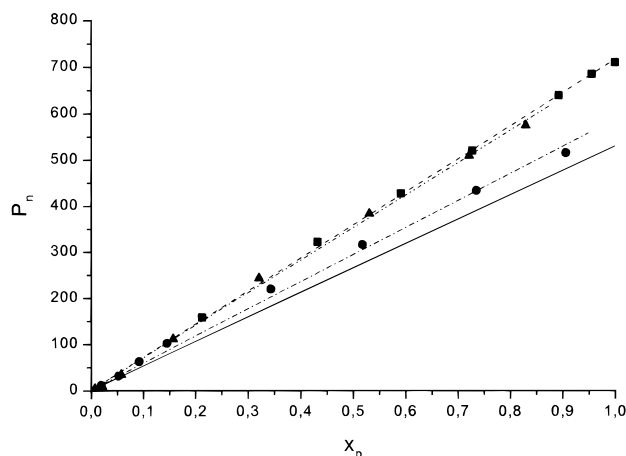


Figure 4. Plot of the number-average degree of polymerization, \bar{P}_n , vs monomer conversion, x_p , for the polymerizations described in Figure 3. Key: (—) calculated $\bar{P}_n = x_p[\text{MMA}]_0/[\text{EiBLi}]_0$.

Effect of the Complex Concentration. The first-order time-conversion plots are only linear when a sufficiently high concentration of the $\text{NBu}_4^+[\text{Al}_2\text{Et}_6\text{Br}]^-$ complex is used. Otherwise, the value of the apparent rate constant of propagation, k_{app} , increases during the

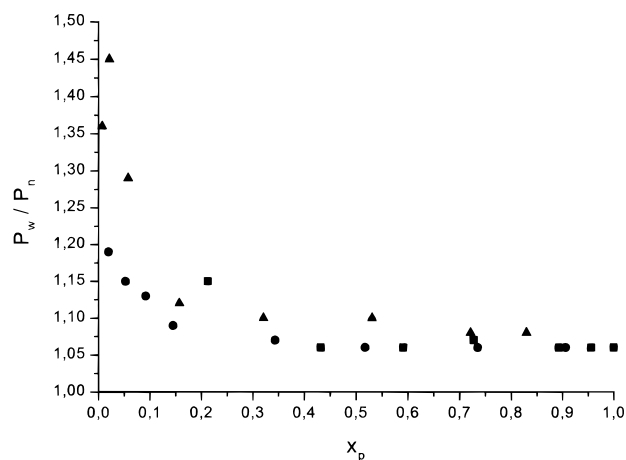


Figure 5. Plot of the polydispersity index, \bar{P}_w/\bar{P}_n , vs monomer conversion, x_p , for the polymerizations described in Figure 3.

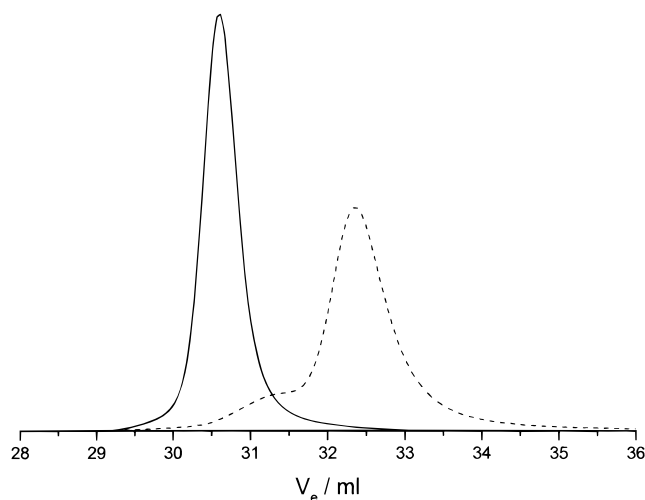


Figure 6. GPC eluograms of the polymers obtained from the anionic polymerization of MMA with $\text{EiBLi}/\text{NBu}_4^+[\text{Al}_2\text{Et}_6\text{Br}]^-$ (▲ in Figure 3) at $x_p = 0.06$ (—, $\bar{M}_w/\bar{M}_n = 1.29$) and $x_p = 0.32$ (---, $\bar{M}_w/\bar{M}_n = 1.10$).

early stages of the polymerization and is then constant (cf. Figure 3). Even then, the plots of \bar{P}_n vs conversion are linear (cf. Figure 4), so that this observation can hardly be explained by a slow initiation process. The molecular weight distributions of the polymers are, however, bimodal at first but unimodal and narrow for higher monomer conversions (cf. Figures 5 and 6). It

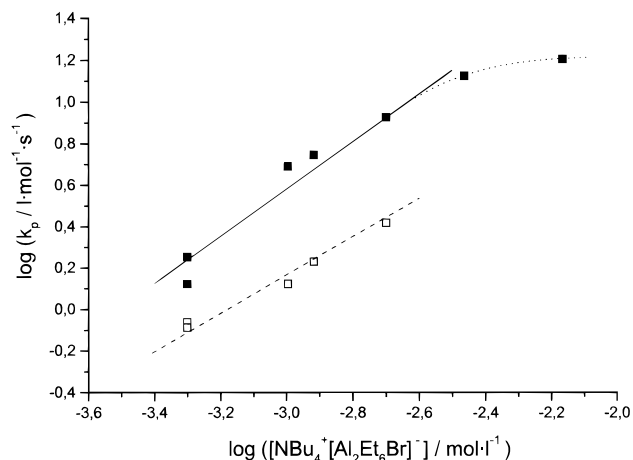
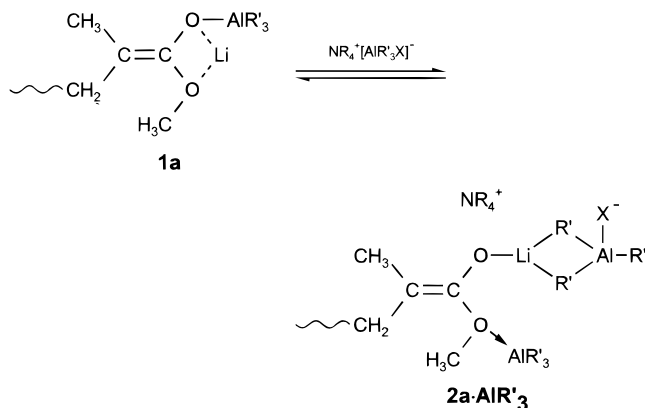


Figure 7. Determination of the reaction order with respect to the concentration of the tetrabutylammonium bromide-triethylaluminum complex, $[\text{NBu}_4^+][\text{Al}_2\text{Et}_6\text{Br}]^-$. For reaction conditions, see Figure 3. Slopes: 0.9 ± 0.1 (k'_p , \square), 1.1 ± 0.1 (k_p , \blacksquare).

Scheme 2. Equilibrium between the Active Species 1 and 2 (Dimeric Structures Omitted)



seems therefore reasonable to consider an equilibrium between various active species of different reactivity.

From the initial and the final slopes of the curved first-order time-conversion plots, we can calculate two rate constants of propagation, k'_p and k_p , respectively. The bilogarithmic plot of these rate constants vs the concentration of the tetrabutylammonium bromide-triethylaluminum complex, $[\text{NBu}_4^+][\text{Al}_2\text{Et}_6\text{Br}]^-$, (Figure 7) shows that, in both stages, the polymerization follows first-order kinetics with respect to the complex concentration. Regarding the initial stage, it is found that the linear plot of k'_p vs $[\text{NBu}_4^+][\text{Al}_2\text{Et}_6\text{Br}]^-$ has an intercept of $k'_p = 0.13 \text{ l mol}^{-1} \text{ s}^{-1}$ —this value is close to that of the rate constant which was determined in the absence of the tetrabutylammonium bromide ($k_p = 0.08 \text{ l mol}^{-1} \text{ s}^{-1}$ at -23°C).³

Therefore, we consider an equilibrium between **1** and **2** (or its AlR'_3 adduct) with the latter as the more reactive species (Scheme 2). If this equilibrium shifts toward **2** with increasing concentration of the $\text{NBu}_4^+[\text{Al}_2\text{Et}_6\text{Br}]^-$ complex, the polymerization will follow the observed first-order kinetics. To explain the increasing slope of the first-order time-conversion plots, we suppose that the equilibrium position and/or the degree of association of the living chains depend on their degree of polymerization. It has been frequently observed that low molecular weight ester enolates behave differently from the corresponding polymer chain ends. As an

example, methyl α -(tetraphenylphosphonium)isobutyrate, MiB^-TPP^+ , has a higher tendency than $\text{PMMA}^-\text{TPP}^+$ to form unreactive phosphor ylides.¹³ As the molecular weight distributions of the polymers obtained in the early stage of the polymerization are broad, the establishment of the equilibrium between **1** and **2** or dissociation of dimeric associates should be slow with respect to propagation.¹⁴ For high complex concentrations, $[\text{NBu}_4^+][\text{Al}_2\text{Et}_6\text{Br}]^-/[\text{P}^*]_0 > 6$, we obtain linear first-order time-conversion plots and the reaction approaches zeroth order with respect to the complex concentration (cf. Figure 7). This might suggest that the equilibrium in Scheme 2 is then totally shifted toward **2**.

Effect of other Tetraalkylammonium Halides.

The use of various $\text{NR}_4^+[\text{Al}_2\text{Et}_6\text{X}]^-$ complexes ($\text{R} = \text{Me}, \text{Et}, \text{Bu}$; $\text{X} = \text{Cl}, \text{Br}, \text{I}$) at high concentrations leads to linear first-order time-conversion plots.⁸ It was found that the rate of propagation increases with increasing size of the tetraalkylammonium ion.⁹ Indeed, with regard to the structure of **2** in Chart 1, one would expect that the radius of the tetraalkylammonium gegenion affects the interionic distance to the carbanion and thus the reactivity of the active species. Surprisingly, the rate of propagation decreases with increasing size of the halide.⁹ This observation can hardly be explained with structure **2** because of the large distance between the halide and the carbanion. It appears that we have to take a further active species into account. We assume that **2** might dissociate into a considerably more reactive tetraalkylammonium enolate (or enol aluminate) **3** and a $\text{Li}^+[\text{AlR}'_3\text{X}]^-$ complex (Scheme 3). As the heat of formation of $\text{Li}^+[\text{AlR}'_3\text{X}]^-$ increases with decreasing radius of the halide,⁶ the equilibrium in Scheme 3 will be shifted toward the active species **3**, which should then lead to the observed acceleration of the polymerization. However, the products in Scheme 3 should be considerably less stable than the educts, so that the equilibrium between the active species should lie predominantly on the left-hand side and only a minute fraction of species **3** may be actually formed.

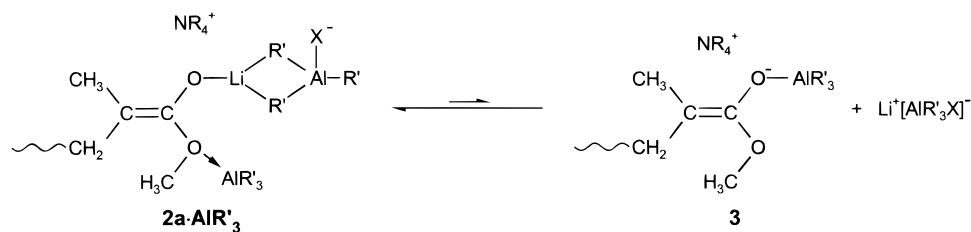
Temperature Dependence. At temperatures below -20°C , we again find slightly curved first-order time-conversion plots (Figure 8), and the polymers obtained at low monomer conversions have bimodal molecular weight distributions. Obviously, the equilibrium in Scheme 2 between **1** and **2** is exothermic; i.e., it shifts to the left-hand side with decreasing temperature (as it does with decreasing concentration of the $\text{NBu}_4^+[\text{Al}_2\text{Et}_6\text{Br}]^-$ complex). At -78°C , we even observe the precipitation of a polymer gel; i.e., then the ester enol aluminate **1** should be the predominant active species.

The Arrhenius plot (Figure 9) of the propagation rate constants, k_p (which were determined from the final slopes in the case of curved first-order time-conversion plots), is linear in the range of -78 to -20°C . The apparent values of the activation parameters are

$$E_a^{\text{app}} = (40.5 \pm 0.9) \text{ kJ/mol} \quad \log A_{\text{app}} = 9.6 \pm 0.2$$

The observed value of the activation energy is much higher than those obtained so far using various counterions and solvents. In toluene, values between 21 and 26 kJ/mol were reported for Li^+ , K^+ , and $\text{Li}^+/\text{AlEt}_3$,^{3,15} whereas in THF the values range from 18 to 24 kJ/mol¹² and a value of 17 kJ/mol is found for group transfer polymerization catalyzed by bifluoride anions.¹⁶ Simi-

Scheme 3. Dissociation of the Active Species 2



$$[P^{(3)}] \propto K_{1-2}K_{2-3}[P^*]$$

where K_{i-j} are the equilibrium constants of the equilibria in Schemes 2 and 3. This leads to the observed propagation rate constant

$$k_p^{\text{obs}} = k_{\text{app}}/[P^*] \approx k_p^{(3)}[P^{(3)}]/[P^*] \propto k_p^{(3)}K_{1-2}K_{2-3}$$

Thus, the observed activation energy obtained from these rate constants will contain the enthalpies for the corresponding equilibria and the frequency exponents will contain the corresponding entropies.

The polymerization of MMA is living up to -20°C only (cf. Table 1). At higher temperatures, the first-order time-conversion plots show a downward curvature indicating the occurrence of termination reactions (cf. Figure 8). Even then, the polymers lack any UV absorption at $\lambda = 300\text{ nm}$, which is characteristic for cyclic β -ketoester end groups. Thus, termination of the living polymer chains via back-biting can be excluded. It is possible that we have to take into account a Hofmann elimination as a termination reaction—this reaction was observed by Bandermann et al.¹⁷ in the polymerization of MMA with tetrabutylammonium malonates in THF.

Tacticities. Independent of the $\text{NR}_4^+[\text{Al}_2\text{Et}_6\text{X}]^-$ complex and with only slight temperature dependence, we obtain syndiotactic polymers—the fraction of racemic triads, rr , is $\sim 75\%$, and that of racemic dyads, r , is $\sim 86\%$ (cf. Table 1). The value of the persistence ratio, ρ , is close to unity, indicating that the monomer addition follows Bernoullian statistics. These results are similar to those found with a cryptated potassium counterion in toluene.¹⁸

Conclusions

The polymerization of MMA with EiBLi in the presence of $\text{NR}_4^+[\text{Al}_2\text{Et}_6\text{X}]^-$ complexes in toluene has a living and controlled character up to -20°C . The reaction follows first-order kinetics with respect to $[P^*]_0$, $[\text{MMA}]_0$, and $[\text{NR}_4^+[\text{Al}_2\text{Et}_6\text{X}]]$, but at low concentrations of the complex, the first-order time-conversion plots are curved, and the polymers are initially bimodal. This is explained by an equilibrium between the active species 1 and 2 (Scheme 2), the position of which establishes rather slowly during polymerization.

The dependence of the propagation rates on the size of both NR_4^+ and X^- can be explained by taking into account some dissociation of 2 to form a tetraalkylammonium enolate 3 (Scheme 3). Decreasing the temperature has a similar effect on kinetics as decreasing the complex concentration.

At this point, we are able to explain all the kinetic results, but we cannot prove the proposed mechanism. Apart from additional kinetic investigations, we are presently studying the structures of active species, e.g.,

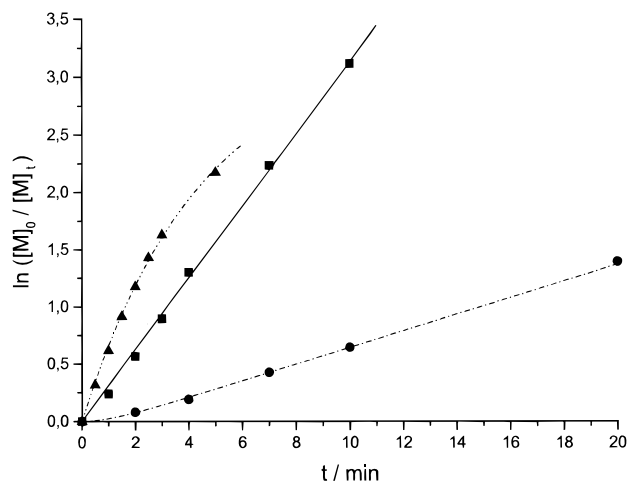


Figure 8. First-order time-conversion plots for the anionic polymerization of MMA with $\text{EiBLi}/\text{NBu}_4^+[\text{Al}_2\text{Et}_6\text{Br}]^-$ in toluene at -38°C (●), -20°C (■), and 0°C (▲). For reaction conditions see Figure 2, $[\text{EiBLi}]_0 = 0.44 \times 10^{-3}\text{ mol/L}$.

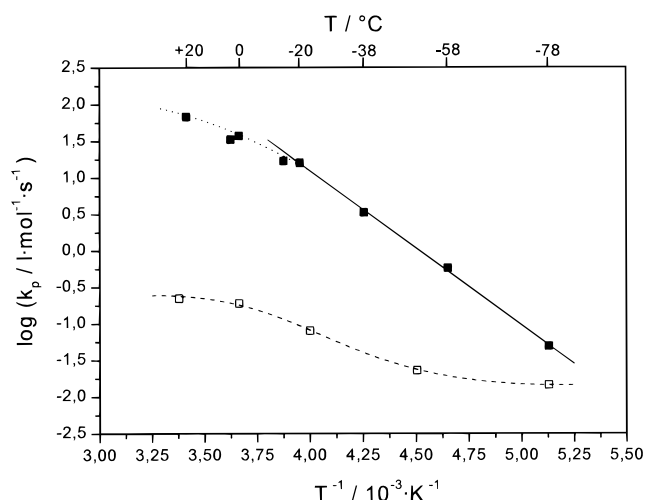


Figure 9. Arrhenius plot for the anionic polymerization of MMA with $\text{EiBLi}/\text{NBu}_4^+[\text{Al}_2\text{Et}_6\text{Br}]^-$ in toluene (■); for reaction conditions see Figure 8. $E_a = (40.5 \pm 0.9)\text{ kJ/mol}$; $\log A = 9.6 \pm 0.2$. Anionic polymerization with $\text{EiBLi}/\text{AlEt}_3$ in 3:1 toluene/methyl pivalate v/v (□), see ref 3.

larly, the values of $\log A$ range from 3 to 7.4. This indicates that the observed activation parameters are apparent values only. If we assume that the polymerization can proceed via three different species, the apparent rate constant is given by

$$k_{\text{app}} = k_p^{(1)}[P^{(1)}] + k_p^{(2)}[P^{(2)}] + k_p^{(3)}[P^{(3)}]$$

If we further assume that the third species is much more reactive than the other ones ($k_p^{(3)} \gg k_p^{(2)}, k_p^{(1)}$), in a first approximation

by NMR measurements and further quantum-chemical calculations.

Acknowledgment. We wish to thank Mrs. Nicole Gilbert and Mr. Peter Blumers for their very helping hands. This work was supported by the Bundesministerium für Bildung, Wissenschaft, Forschung und Technologie and BASF AG, Ludwigshafen, Germany (Project No. 03N 3006 A5).

References and Notes

- (1) Schlaad, H.; Müller, A. H. E. *Macromol. Rapid Commun.* **1995**, *16*, 399.
- (2) Schlaad, H.; Kolshorn, H.; Müller, A. H. E. *Macromol. Rapid Commun.* **1994**, *15*, 517.
- (3) Schlaad, H.; Schmitt, B.; Müller, A. H. E.; Jüngling, S.; Weiss, H. *Macromolecules* **1998**, *31*, 573.
- (4) Weiss, H.; Schlaad, H.; Müller, A. H. E. To be published.
- (5) Schlaad, H.; Müller, A. H. E. *Polym. J.* **1996**, *28*, 954.
- (6) Ziegler, K.; Köster, R.; Lehmkuhl, H.; Reinert, K. *Liebigs Ann. Chem.* **1960**, *629*, 33.
- (7) Natta, G.; Allegra, G.; Perego, G.; Zambelli, A. *J. Am. Chem. Soc.* **1961**, *83*, 5033.
- (8) Schlaad, H. Dissertation, Universität Mainz, 1997.
- (9) Schlaad, H.; Schmitt, B.; Müller, A. H. E. *Angew. Chem.* **1998**, *110*, 1497; *Angew. Chem., Int. Ed. Engl.* **1998**, *37*, 1389.
- (10) Novakov, C. P.; Tsvetanov, C. B. *Macromol. Rapid Commun.* **1995**, *16*, 741.
- (11) Lochmann, L.; Lím, D. *J. Organomet. Chem.* **1973**, *50*, 9.
- (12) Müller, A. H. E. In *Comprehensive Polymer Science*; Allen, G.; Bevington, J. C., Ed., Pergamon: Oxford, England, 1988; Vol. 3, p 387.
- (13) Baskaran, D.; Müller, A. H. E. *Macromolecules* **1997**, *30*, 1869.
- (14) Litvinenko, G.; Müller, A.H. E. *Macromolecules* **1997**, *30*, 1253.
- (15) Piejko, K. E. Dissertation, Universität Bayreuth, 1982.
- (16) Mai, P. M.; Müller, A. H. E. *Makromol. Chem., Rapid Commun.* **1987**, *8*, 247.
- (17) Broska, D.; Fieberg, A.; Heibel, C.; Bander mann, F. *Polym. Prepr. (Am. Chem. Soc., Div. Polym. Chem.)* **1997**, *38* (1), 471.
- (18) Viguier, M.; Collet, A.; Schué, F. *Polym. J.* **1982**, *14*, 137.

MA971854F